Two-stage adaptive PMD compensation experiment for 10-Gb/s optical communication system

Xiaoguang Zhang (张晓光), Li Yu (于 丽), Yuan Zheng (郑 远), Yu Shen (沈 昱), Guangtao Zhou (周光涛), Lin Chen (陈 林), Lixia Xi (席丽霞), Tiecheng Yuan (苑铁成), Jianzhong Zhang (张建忠), and Bojun Yang (杨伯君)

Department of Physics, School of Science, Beijing University of Posts and Telecommunications, Beijing 100876

Received June 26, 2003

We report the adaptive compensation experiment of polarization mode dispersion (PMD) for 10-Gb/s non return-to-zero (NRZ) and return-to-zero (RZ) optical communication systems using a two-stage PMD compensator and the monitoring technique based on degree of polarization (DOP) feedback-signals. The DOP monitor has its advantages of bit-rate independent and modulation format independent. The two-stage compensator has the capacity of compensation for the first- and second-order PMD. The compensated differential group delay (DGD) is up to 80 ps, and compensated principal state of polarization rotation rate is 20 ps. The time used for compensation is less than 1 second.

OCIS codes: 060.2330, 260.5430.

Polarization mode dispersion (PMD) becomes dominant factor of signal degradation in high bit rate (10 Gb/s and beyond) optical communication systems. The adaptive PMD compensation has become a hot topic in recent years[1−7]. The techniques of monitoring PMD in fiber links and control algorithm are most important for a PMD adaptive compensation system. In our previous work, we have successfully realized one-stage PMD adaptive compensation experiments in 2.5-Gb/s[8] and 10-Gb/s[9] return-to-zero (RZ) optical communication systems, in which the technique of observation of the power levels of specific tones in the received radio frequency (RF) spectrum of the base-band signal was used as PMD monitor and the algorithm so-called particle swarm optimization (PSO) was used to control feedback compensation system. In this paper, we report another experiment of adaptive PMD compensation in 10-Gb/s non return-to-zero (NRZ) and RZ transmission systems, in which a two-stage adaptive PMD compensator was used, and another monitoring technique based on degree of polarization (DOP) of the received optical signal was used as feedback signal. The compensator shows the capability to compensate first- and second-order PMD. In the experiment, the local particle swarm optimization (LPSO) was established as control algorithm, which showed powerful ability of fast searching optimism without sinking in sub maxima.

There are mainly two proposed PMD monitoring techniques. One is to observe the power level of specific tones in the received RF spectrum of the base-band signal[1−3]. The other is to evaluate the DOP of optical signal in fiber link[4−7]. In our previous work[8,9], the technique of specific tones in the received RF spectrum was used as feedback signal.

The basic structure of PMD monitoring technique based on DOP is shown in Fig. 1. The DOP monitor has only a polarimeter which is bit-rate independent and modulation format independent. Because its merits of bit-rate independent and hardware simplicity, we choose DOP evaluation as feedback signals in this experiment.

For a DOP monitor, a polarimeter is used to judge the states of polarization of light in fiber link through measuring the Stokes parameters s_0, s_1, s_2, s_3. The DOP is calculated by

$$\mathrm{DOP} = \frac{\sqrt{s_1^2 + s_2^2 + s_3^2}}{s_0}. \tag{1}$$

We have measured DOP versus the differential group delay (DGD) for RZ and NRZ modulation formats with power splitting ratio $\gamma = 0.5$, as shown in Fig. 2. It shows that DOP could be a good indicator of PMD and modulation format independent.

In order to improve accuracy of DOP measurement, we adopted two filtering techniques to eliminate noise from fiber link and A/D converters. One is electrical Butterworth low-pass filters before A/D converters. The other is digital filtering technique, which is called median

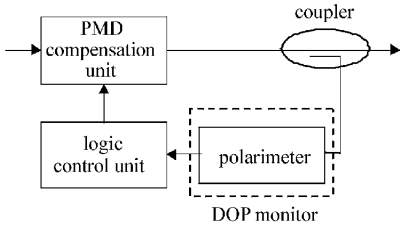

Fig. 1. The structure of PMD monitoring technique based on DOP.

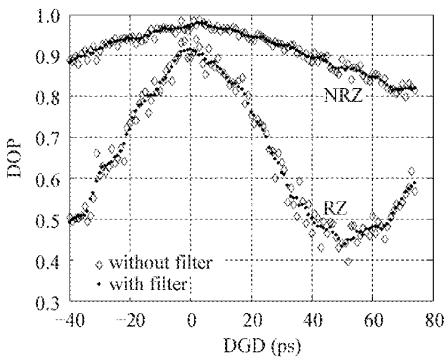

Fig. 2. The experimental results of DOP versus DGD for 10-Gb/s NRZ and RZ formats ($\gamma = 0.5$).

filtering commonly used in image processing. The digital filtering is made with collecting 20 DOP data in each group. The effectiveness of filtering techniques is shown in Fig. 2.

One kind of PMD emulators is made of several lengths of polarization maintaining fiber (PMF) connected through polarization controllers. For the reason of large insertion loss induced by multi-splices and connectors, we adopted two-section emulator as shown in Fig. 3(a), which is the simplest model just including second-order PMD. It provides total first-order PMD vector $\vec{\tau}_e$ and second-order PMD vector $\vec{\tau}_{e\omega}$ in Stokes space as follows[10]

$$\vec{\tau}_e = \Delta\tau_e \hat{p}_e = R_{e2}\vec{\tau}_{e1} + \vec{\tau}_{e2} = \sqrt{\Delta\tau_{e1}^2 + \Delta\tau_{e2}^2 + 2\Delta\tau_{e1}\Delta\tau_{e2}\cos\theta}\,\hat{p}_e, \quad (2)$$

$$\vec{\tau}_{e\omega} = \Delta\tau_{e\omega}\hat{p}_e + \Delta\tau_e\hat{p}_{e\omega} = \Delta\tau_e\hat{p}_{e\omega} = \vec{\tau}_{e2} \times R_{e2}\vec{\tau}_{e1} = \Delta\tau_{e1}\Delta\tau_{e2}\sin\theta\hat{p}_{e\omega}/|\hat{p}_{e\omega}|, \quad (3)$$

where $\Delta\tau_e$ is the total DGD of the emulator, $\hat{p}_e$ is the unit vector pointing in the direction of slower principal state of polarization (PSP) in Stokes space. $\vec{\tau}_{e1}$ and $\vec{\tau}_{e2}$ are PMD vectors of first and second PMF, respectively. R_{e1} is the Müller rotation matrix of the first PMF, whereas R_{e2} is the Müller rotation matrix of the second PMF combined with the PC. Note that these rotations only change the orientation of PMD vectors without changing their magnitudes. θ is the angle between $R_{e2}\vec{\tau}_{e1}$ and $\vec{\tau}_{e2}$. In Eq. (3), the subscript ω indicates differentiation with respect to ω. The total second-order PMD vectors of the emulator can be divided into two orthogonal components $\Delta\tau_{e\omega}\hat{p}_e$ (along the direction of $\vec{\tau}_e$) and $\Delta\tau_e\hat{p}_{e\omega}$ (perpendicular to $\vec{\tau}_e$), in which the $\Delta\tau_{e\omega}$ is the change rate of DGD with ω (called polarization-dependent chromatic dispersion (PCD)), while $\hat{p}_{e\omega}$ is the change rate of PSPs with ω (called PSP rotation rate (PSPrr)).

The total DGD of the emulator can range from $|\Delta\tau_{e1} - \Delta\tau_{e2}|$ to $\Delta\tau_{e1} + \Delta\tau_{e2}$ through adjusting PC, as shown in Fig. 3(c), in which $\Delta\tau_{e1} = 60$ ps and $\Delta\tau_{e2} = 20$ ps. In addition, we can see that for two-section emulator the second-order PMD vector has only component related with PSPrr, as shown in Fig. 3(b). The magnitude of $\hat{p}_{e\omega}$ for the emulator ranges from -20 to 20 ps, as shown in Fig. 3(c).

References [10] and [11] have pointed that the PSPrr resulted in pulse overshoots and the generation of satellite pulses for NRZ format, which also appeared in our experiment as discussed as follows. For real fiber link, PCD is the minor component of the second-order PMD vector and makes less impairment to systems, while the orthogonal components is the larger component and the dominant impairment factor to systems[10]. In this point of view, the two-section emulator used in the experiment is acceptable.

It is well known that two-stage compensators are able to compensate also for high order PMD[12]. Figure 4 shows the two kinds of schemes of two-stage compensator, which have 4 or 5 control parameters or degrees of freedom (DOFs) according to the second delay line used is fixed or variable. In our experiment we choose two-stage with two fixed delay lines because the variable

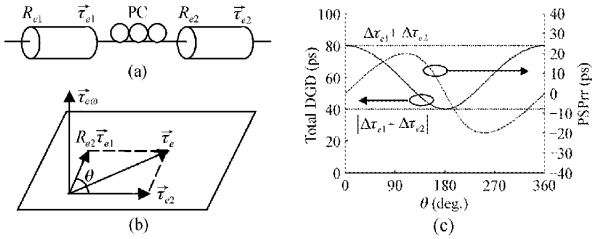

Fig. 3. (a) Two-section PMD emulator, (b) the second-order PMD vector of the emulator, (c) total DGD and PSPrr of the emulator.

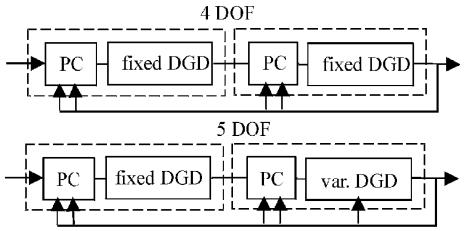

Fig. 4. Two-stage compensator scheme.

delay line we have is slow to adjust (about 3 ps/s). Besides, our choice has less DOF and is easier to control.

The compensation theory of the two-stage compensators shown in Fig. 4 is described as follows. The total first- and second-order PMD vectors in fiber link including the emulator and two-stage compensator can be written as

$$\vec{\tau}_{\rm tot} = R_{c2}R_{c1}[\vec{\tau}_e + R_{c1}^{\dagger}(\vec{\tau}_{c1} + R_{c2}^{\dagger}\vec{\tau}_{c2})], \quad (4)$$

$$\vec{\tau}_{{\rm tot}\omega} = R_{c2}R_{c1}\left\{\vec{\tau}_{e\omega} + [R_{c1}^{\dagger}(\vec{\tau}_{c1} + R_{c2}^{\dagger}\vec{\tau}_{c2})] \times \vec{\tau}_e + R_{c1}^{\dagger}[(R_{c2}^{\dagger}\vec{\tau}_{c2}) \times \vec{\tau}_{c1}]\right\}, \quad (5)$$

where $\vec{\tau}_{c1}$ and $\vec{\tau}_{c2}$ are the first-order PMD vectors of the two stages of compensator, respectively. The R_{c1} and R_{c2} are the Müller rotation matrixes of two stages. The superscript "†" denotes their Herimitian conjugation matrixes. $R_{c1}^{\dagger}[(R_{c2}^{\dagger}\vec{\tau}_{c2}) \times \vec{\tau}_{c1}]$ can be explained as such a process: two vectors carry out a multiplication cross operation and then the resultant vector is rotated by an angle. This process is equivalent to that the two vectors are rotated by the same angle at first and then carry out a multiplication cross operation, as can be expressed by $(R_{c1}^{\dagger}R_{c2}^{\dagger}\vec{\tau}_{c2}) \times (R_{c1}^{\dagger}\vec{\tau}_{c1})$. Let $\vec{a} = R_{c1}^{\dagger}R_{c2}^{\dagger}\vec{\tau}_{c2}$ and $\vec{b} = R_{c1}^{\dagger}\vec{\tau}_{c1}$, whose lengths $|\vec{a}| = |\vec{\tau}_{c2}| = \Delta\tau_{c2}$ and $|\vec{b}| = |\vec{\tau}_{c1}| = \Delta\tau_{c1}$, respectively, are DGDs of two stages. Therefore, the magnitudes of total first- and second-order PMD vectors are

$$|\vec{\tau}_{\rm tot}| = |\Delta\tau_e\hat{p}_e + \vec{a} + \vec{b}|, \quad (6)$$

$$|\vec{\tau}_{{\rm tot}\omega}| = |\Delta\tau_e\hat{p}_{e\omega} + (\vec{a} + \vec{b}) \times (\Delta\tau_e\hat{p}_e) + \vec{a} \times \vec{b}|. \quad (7)$$

For two-stage compensator, the operation of simultaneous compensation for the first- and second-order PMD of the emulator can be expressed by Eqs. (6), (7), and

Fig. 5. In Eq. (6), in order to compensate the first-order PMD, we must adjust the compensator to obtain

$$\vec{a} + \vec{b} = -\Delta\tau_e \hat{p}_e, \tag{8}$$

which is in the opposite direction of emulator's first-order PMD vector $\vec{\tau}_e$, with the result that the second term in Eq. (7) vanishes. Therefore, $|\vec{\tau}_{\mathrm{tot}\omega}| = |\Delta\tau_e \hat{p}_{e\omega} + \vec{a} \times \vec{b}|$. If we let $\vec{a}$ and $\vec{b}$ are placed in the plane P which consists of $\hat{p}_e$ and $\hat{p}_e \times \hat{p}_{e\omega}$, as shown in Fig. 5, the direction of $\vec{a} \times \vec{b}$ is perpendicular to plane P and points opposite to PSPrr $\Delta\tau_e \hat{p}_{e\omega}$. The condition for eliminating PSPrr is

$$\vec{a} \times \vec{b} = -\Delta\tau_e \hat{p}_{e\omega}. \tag{9}$$

Although the two-stage compensator with 4 DOFs has fixed DGDs of $\Delta\tau_{c1} = |\vec{b}|$ and $\Delta\tau_{c2} = |\vec{a}|$, we can adjust the angle between $\vec{a}$ and $\vec{b}$ to closely satisfy the Eqs. (8) and (9) at the same time. If the DGD of second stage delay line is variable, we can exactly satisfy the Eqs. (8) and (9) simultaneously which means that the first- and second-order PMD can be compensated completely.

In adaptive PMD compensator, one of the main key factors that determine the speed of compensation is the control algorithm. In the related literatures[1,2,4–6], the control algorithm has not been mentioned. References [3] and [7] report the algorithm used for control is a gradient peak search method. In our opinion, when the numbers of control parameters (DOFs) increase, this control algorithm may sometimes lock into sub-maxima (sub-optima for compensation) rather than finding out the global-maximum (optimum for compensation). Besides, the gradient based algorithm would less effective for low signal noise ratio (SNR) optical communication systems because the information of gradient between neighboring signals would be submerged in noise. In our previous work[8,9], we used an artificial intelligence searching algorithm, called PSO, in automatic PMD compensation. In our present work, we improved our PSO algorithm, and established another PSO algorithm called LPSO, which has many advantages: fast and powerful capacity of searching the global-optimum without sinking into sub-optima (especially for the situation of many DOFs to be controlled), powerful capacity of noise resistance which fits for low SNR systems. A good control algorithm must realize two functions: an optimized maximum searching and continuously tracking the optimum. For tracking mode we used the method of slight disturbances or dithering when the optimum condition changed.

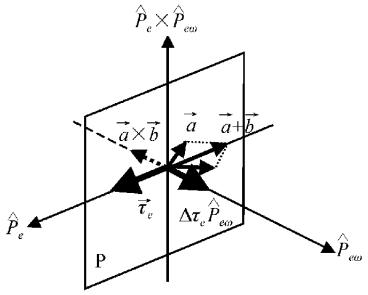

Fig. 5. The operation mode for compensating the first- and second-order PMD, in which $\vec{a}$ and $\vec{b}$ are placed in the plane P and $\vec{a} \times \vec{b}$ (dashed arrow) is perpendicular to plane P.

Figure 6 shows the experiment setup of our two-stage adaptive PMD compensator for a 10-Gb/s optical communication system. A 1551.8-nm distributed feedback laser is driven externally with 10-Gb/s $2^{23} - 1$ pseudo-random bit sequence using an electro-absorption modulator for NRZ format generation and the combination of an EA and a MZ-$LiNbO_3$ modulator for RZ format generation. The PMD emulator consists of two-section units of two manually adjusted polarization controllers (PC#1 and PC#2) and two polarization maintaining fibers pieces (PMF#1 and PMF#2) of 60 and 20 ps DGDs. The PMD emulator generates DGD of about $40 - 80$ ps measured by Sagnac interferometer[13]. The PSPrr is estimated from -20 to 20 ps according to Eq. (3) and Fig. 3(c). For two-stage PMD compensator, each stage has an electrically controlled polarization controller and a delay line. The first electrically controlled polarization controller PC#3 (from General Photonics Co.) has four fiber-squeezer cells to be adjusted with $0 - 10$ V voltage, out of which only two cells are used in the experiment. The second electrically controlled polarization controller PC#4 (from Corning Co.) has four electro-optic crystal cells adjusted with $0 - 4$ V voltage, out of which only two cells are used in the experiment. The delay line #1 is a PMF with 29 ps DGD, and delay line #2 is an air gap delay line which produces a DGD of 50 ps by adjusting the length of air gap. In received end, an in-line polarimeter is used to measure instantaneously the Stokes parameters s_0, s_1, s_2, s_3, and DOPs as the feedback signals, in which we use two filtering methods for measurement accuracy as explained above. The logic control unit adjusts the four cells of PC#3 and PC#4 to search and track the optimum of the PMD compensator by using LPSO algorithm according to the DOP signals in fiber link. The effectiveness of PMD compensation is observed by eye diagram on the oscilloscope.

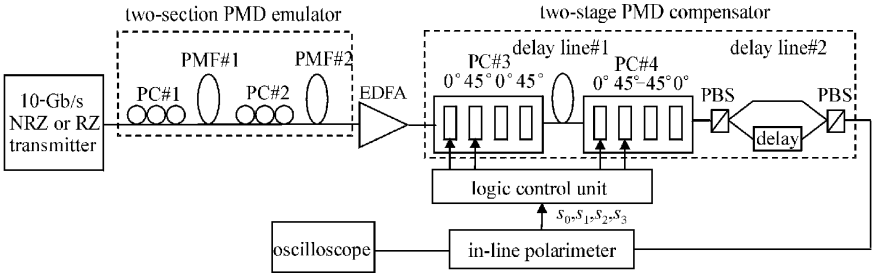

Fig. 6. Experimental setup. PC: polarization controller; PMF: polarization-maintaining fiber; EDFA: erbium-doped fiber amplifier; PBS: polarization beam splitter.

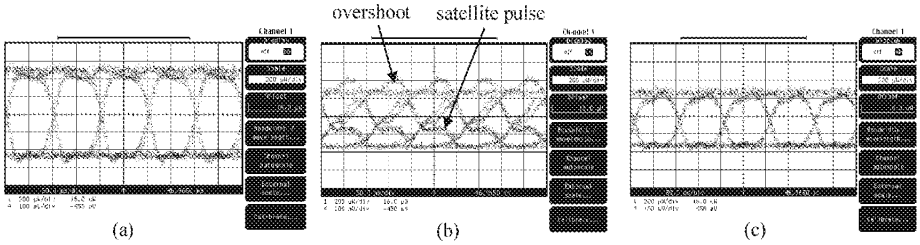

Fig. 7. Eye diagrams to show the procedure of adaptive PMD compensation for 10-Gb/s NRZ optical communication system. (a) Back-to-back, (b) without PMD compensation, (c) with PMD compensation.

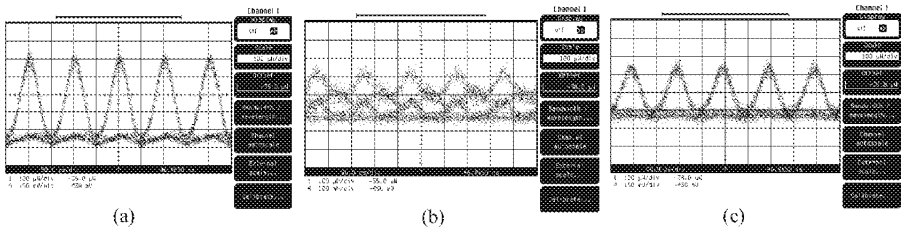

Fig. 8. Eye diagrams to show the procedure of adaptive PMD compensation for 10-Gb/s RZ optical communication system. (a) Back-to-back, (b) without PMD compensation, (c) with PMD compensation.

The whole procedure of adaptive PMD compensation was observed with the oscilloscope. Figures 7 and 8 show the effectiveness of our adaptive PMD compensator by eye diagrams for 10 Gb/s NRZ and RZ formats, respectively. Figures 7(a) and 8(a) show the eye diagrams of back-to-back 10-Gb/s NRZ and RZ formats, respectively. When we adjusted the wave plates of PC#1 and PC#2 of PMD emulator, the worst eye diagrams would be shown on oscilloscope. Figures 7(b) and 8(b) show these saturations for NRZ and RZ formats, respectively. The clear overshoots and satellite pulses phenomena can be seen in Fig. 7(b), which were induced apparently by second-order component relating to PSPrr. When the PMD compensator was switched on, the eye diagrams opened in less than 1 second searching optimum by logic control unit (Fig. 7(c) for NRZ and Fig. 8(c) for RZ formats). The compensation time was measured with a timer set in computer. The good eye diagrams were obtained after compensation even though the PSPrr exists, which confirmed our two-stage compensation can compensate PMD up to second-order. Afterward, when we randomly rotated one of the wave plates of PC #1 or PC #2 at the speed of roughly estimated 20°/second, the eye diagrams remained open all the time, which confirmed the effectiveness of our PMD tracking algorithm.

We have theoretically analyzed PMD characteristics of two-section PMD emulator and operation mode for compensating the first- and second-order PMD. We have also carried out successfully the experiment of adaptive PMD compensation with two-stage compensator showing a capability to automatically compensate the first- and second-order PMD. In our experiment, the DOP monitoring technique was used as feedback-signals, and LPSO algorithm and method of slight disturbances or dithering were used for optimum searching and tracking.

This work was supported by the National "863" High Technology Project (2001AA122041) and the National Natural Science Foundation of China (60072042). X. Zhang's e-mail address is xgzhang@bupt.edu.cn.

References

1. T. Takahashi, T. Imai, and M. Aiki, Electron. Lett. **30,** 348 (1994).
2. F. Heismann, D. A. Fishman, and D. L. Wilson, in *Proceedings of ECOC'98* WdC11, 529 (1998).
3. R. Noé, D. Sandel, M. Yoshida-Dierolf, S. Hinz, V. Mirvoda, A. Schöpflin, C. Glingener, E. Gottwald, C. Scheerer, G. Fischer, T. Weyrauch, and W. Haase, J. Lightwave Technol. **17,** 1602 (1999).
4. C. Francia, F. Bruyère, J.-P. Thiery, and D. Penninckx, Electron. Lett. **35,** 414 (1999).
5. N. Kikuchi, J. Lightwave Technol. **19,** 480 (2001).
6. J. C. Rasmussen, A. Isomura, and G. Ishikawa, J. Lightwave Technol. **20,** 2101 (2002).
7. J. C. Rasmussen, in *2003 Digest of the LEOS Summer Topical Meetings* 47 (2003).
8. X. G. Zhang, L. Yu, Y. Zheng, C. Y. Li, G. T. Zhou, Y. Shen, B. J. Yang, H. X Wang, L. Wang, and Y. F. Ji, Acta Photon. Sin. (in Chinese) (to be published).
9. X. G. Zhang, L. Yu, G. T. Zhou, Y. Shen, Y. Zheng, C. Y. Li, Y. M. Liu, L. Chen, and B. J. Yang, Chin. Opt. Lett. **1,** 447 (2003).
10. H. Kogelnik and R. M. Jopson, in *Optical Telecommunications IVB* (I. P. Kaminow and T. Li, eds.) (Academic Press, San Diego, 2002) chap. 15.
11. C. Francia, F. Bruyère, D. Pennickx, and M. Chbat, IEEE Photon. Technol. Lett. **10,** 1739 (1998).
12. H. Sunnerud, C. Xie, M. Karlsson, R. Samuelsson, and P. A. Andrekson, J. Lightwave Technol. **20,** 368 (2002).
13. X. M. Liu, C. Y. Li, R. H. Li, B. J. Yang, and X. G. Zhang, Chin. J. Lasers (in Chinese) **29,** 455 (2002).